



HAL
open science

Effect of the Si excess on the structure and the optical properties of Nd-doped Si-rich silicon oxide

Chuan-Hui Liang, Olivier Debieu, Yong-Tao An, Larysa Khomenkova, Julien Cardin, Fabrice Gourbilleau

► **To cite this version:**

Chuan-Hui Liang, Olivier Debieu, Yong-Tao An, Larysa Khomenkova, Julien Cardin, et al.. Effect of the Si excess on the structure and the optical properties of Nd-doped Si-rich silicon oxide. *Journal of Luminescence*, 2012, 132 (12), pp.3118-3121. 10.1016/j.jlumin.2012.01.046 . hal-00736631v2

HAL Id: hal-00736631

<https://hal.science/hal-00736631v2>

Submitted on 25 Oct 2017

HAL is a multi-disciplinary open access archive for the deposit and dissemination of scientific research documents, whether they are published or not. The documents may come from teaching and research institutions in France or abroad, or from public or private research centers.

L'archive ouverte pluridisciplinaire **HAL**, est destinée au dépôt et à la diffusion de documents scientifiques de niveau recherche, publiés ou non, émanant des établissements d'enseignement et de recherche français ou étrangers, des laboratoires publics ou privés.

Effect of the Si excess on the structure and the optical properties of Nd-doped Si-rich silicon oxide

C.-H. Liang, O. Debieu, Y.-T. An, L. Khomenkova, J. Cardin*, F. Gourbilleau

CIMAP, UMR CNRS/CEA/ENSICAEN/UCBN, Ensicaen, 6 Bd Maréchal Juin, 14050 Caen Cedex 4, France

ABSTRACT

Nd-doped Si-rich silicon oxide thin films were produced by radio frequency magnetron co-sputtering of three confocal cathodes: Si, SiO₂, and Nd₂O₃, in pure argon plasma at 500 °C. The microstructure and optical properties of the films were investigated versus silicon excess and post-deposition annealing treatment by means of ellipsometry and Fourier transform infrared spectrometry as well as by the photoluminescence method. A notable emission from Nd³⁺ ions was obtained for the as-deposited sample, while the films annealed at 900 °C showed the highest peak intensity. The maximum emission was observed for the films with 4.7 at% of Si excess.

Keywords:

Si-rich-silicon oxide
Neodymium
Magnetron sputtering
Refractive index
Infrared absorption
Photoluminescence

1. Introduction

During last decade a great research effort has been focused on the development of the Si-based nanostructured materials for photonic application [1–5]. Among them, Si nanoclusters (Si-ncs) embedded in SiO₂ host are widely studied due to an achievement of room-temperature light emission from the blue to the infrared depending on the Si-ncs size [6,7].

Rare-earth (RE) ions possess narrow emission lines and receive more and more interest from the scientists in the world [8]. RE doped silica is a well-known medium for laser application, but its use requires high-power sources to achieve an efficient emission. Considerable attention was paid to silica co-doped with RE ions and Si-ncs since (i) such nanocomposite materials can be pumped using broadband sources due to the spectrally wide absorption of Si-ncs and (ii) Si-ncs are found to be efficient sensitizers of RE ions.

In this regard, the most studied materials are Er-doped Si-rich silicon oxide (SRSO) due to promising application as a source for optical communication. In previous works [9–15] a significant enhancement of photoluminescence (PL) intensity of the intra-4f shell transition of Er³⁺ due to the energy transfer from Si-ncs to RE ions has been demonstrated. The detailed study of the excitation mechanism of Er³⁺ ions showed that the excitation rate depends on the Si-ncs size and becomes higher for the smaller Si-ncs [16].

In the contrast of well-studied Er-SRSO system, other RE ions are not well-addressed. On the contrary to Er³⁺ ions, the doping

of SRSO with Nd³⁺ ions is most promising due to overlapping of 4f-shell absorption transitions with the range of intrinsic Si-ncs PL. Moreover, Nd³⁺ ions offer very important light emission in the infrared spectral range at 1.06 and 1.32 μm in a four-level system configuration which avoid re-absorption of the emitted radiation. The benefits of Si-nc sensitizers towards Nd³⁺ ions was already demonstrated [17,18]. However, its improvement requires a special attention to some critical parameters as the coupling rate between Nd³⁺ ions and Si-ncs as well as the quality of the surrounded host medium aiming significant decrease of the non-radiative channels contribution. In the former case, the coupling rate can be monitored via the Nd³⁺ ions content and the Si excess (Si_{ex}) concentration. The latter has a direct influence on the number of Si-ncs embedded in SiO₂ as well as on the host quality.

In this study, both the structure and the optical properties of Nd-doped SRSO thin films were investigated versus Si_{ex} and the annealing treatment in order to obtain high efficient of Nd³⁺ light emission via energy transfer from Si-ncs toward Nd³⁺ ions.

2. Experimental techniques

The samples were deposited onto p-type silicon wafers by radio frequency magnetron co-sputtering of three confocal cathodes: Si, SiO₂, and Nd₂O₃, in a pure argon plasma. The substrate was rotated during the deposition to ensure a high homogeneity of the film. The deposition temperature and the total plasma pressure were kept at 500 °C and 3 mTorr, respectively. The power density applied on the SiO₂ and the Nd₂O₃ cathodes were fixed at 8.88 and 0.30 W/cm², respectively, whereas the power density applied on the Si cathode, P_{Si}, was varied from 0.74 to

* Corresponding author.

E-mail address: julien.cardin@ensicaen.fr (J. Cardin).

2.37 W/cm². The deposition time was tuned to achieve the film thickness in the 250–300 nm range for avoiding the effect of the film stresses on the optical parameters [19]. An annealing treatment was performed in a conventional furnace at 900 and 1100 °C during 1 h in a nitrogen flow. Spectroscopic ellipsometry was used to determine the optical constants: thickness and refractive index n of the films. The data were collected by means of a Jobin–Yvon ellipsometer (UVISSEL) where the incident light was scanned in the 1.5–4.5 eV range under an incident angle of 66.3°. The fitting of the experimental data was performed using DeltaPsi2 software [20].

The sample's infrared absorption properties were investigated by means of a Nicolet Nexus Fourier transform infrared (FTIR) spectrometer. The spectra were acquired under normal and Brewster angle incidence (65°). The PL spectra were recorded with a photomultiplier tube Hamamatsu (R5108) after dispersion of the PL signal with a Jobin–Yvon TRIAX 180 monochromator using an Ar⁺ laser operated at 488 nm which is a non-resonant wavelength for Nd³⁺ excitation. For this study, we focused our PL experiment in the visible-near infrared range (600–1000 nm) to analyze the unique contribution of the RE ions in the de-excitation process [17].

3. Results and discussion

3.1. The Si_{ex} estimation

Fig. 1 displays the evolutions of the refractive index n and the TO₃ peak position of Si–O vibration bond as a function of P_{Si} for as-deposited samples. The n value increases from 1.48 to 1.70 with P_{Si} . According to the effective medium approximation (EMA) and using the Bruggeman model theory [21–23], the O/Si ratio (x) can be determined from the following equation:

$$x = \frac{-36n^4 + 691n^2 + 773}{22n^4 + 665n^2 - 472} \quad (1)$$

To note that the n value is given at 1.95 eV, and during the deducing of Eq. (1), $n_{a-si} = 4.498$ and $n_{SiO_2} = 1.457$ are used.

Furthermore, the peak position of the TO₃ mode in Fig. 1 decreases almost linearly with the increased P_{Si} . On the basis of the following equation [24]:

$$x = 0.02v - 19.3 \quad (2)$$

v is the TO₃ peak position of sample SiO _{x} , one can obtain the x value. For this pure SiO₂ layer was grown at the same conditions as SRSO–Nd layers and had the same thickness. This approach gives more accurate estimation than the comparison with the TO₃ peak position of SiO₂ (~1080 cm⁻¹) published elsewhere [25].

Thereafter, Si_{ex} (at%) was calculated from x using the following equation:

$$Si_{ex}(\text{at}\%) = \frac{2-x}{2+2x} 100 \quad (3)$$

And the results of Si_{ex} estimated from both FTIR and EMA are shown in Fig. 2. It is worth to note that the Si_{ex} values obtained by the two methods are in good agreement within uncertainty.

3.2. Effect of annealing treatment on the microstructure

Fig. 3 shows a typical evolution of the FTIR spectra recorded at the Brewster incidence for films ($P_{Si} = 1.33$ W/cm²) as-deposited and annealed at 900 and 1100 °C. This film was chosen as a typical one to study for its highest emission from Nd³⁺ ions discussed later. The spectra are normalized with respect to the TO₃ phonon mode intensity. It is found that the TO₃ peak position shifts from 1050 to 1080 cm⁻¹ with the increasing annealing temperature (T_A). This great shift is explained by the condensation and agglomeration of the Si_{ex} resulting in the formation of Si–ncs [26] at the expense of volumic silica. The evolution of FTIR spectra is a confirmation of the formation of SiO₂ and Si phases via phase separation in the SiO _{x} host [25]. Moreover, the intensity of the LO₃ peak increases and the intensity of the LO₄–TO₄ pair mode attenuates with the increase of T_A . The former is a signature of the improvement of the Si/SiO _{x} interface [27], whereas the latter indicates a reduction in disorder of the host.

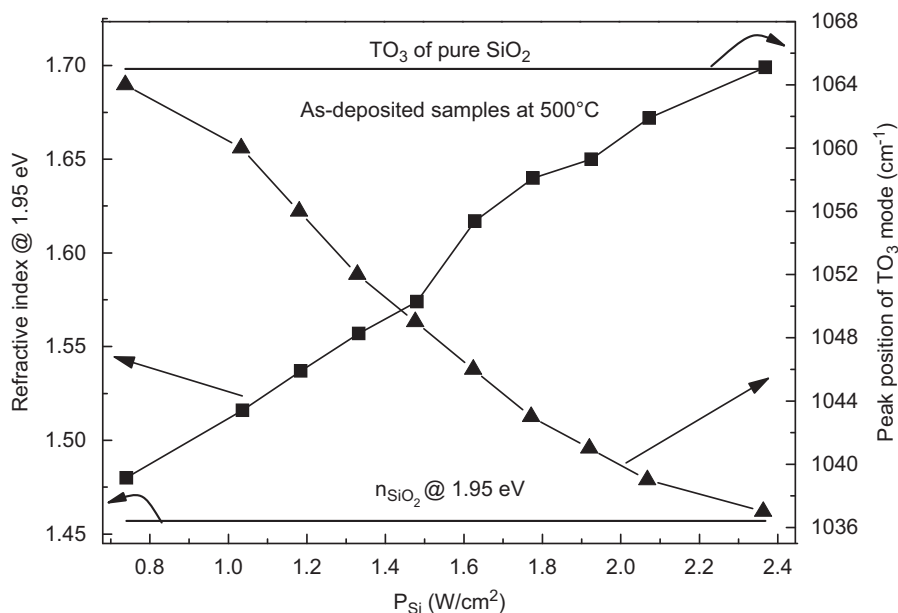


Fig. 1. Evolution of the refractive index n taken at 1.95 eV energy (left axis) and of the TO₃ Si–O peak position (right axis) versus P_{Si} for as-deposited samples. The lines on top and bottom are the TO₃ position (1065 cm⁻¹) and the refractive index n (1.457) for pure SiO₂ grown at the same conditions with the same thickness as SRSO–Nd layers, respectively.

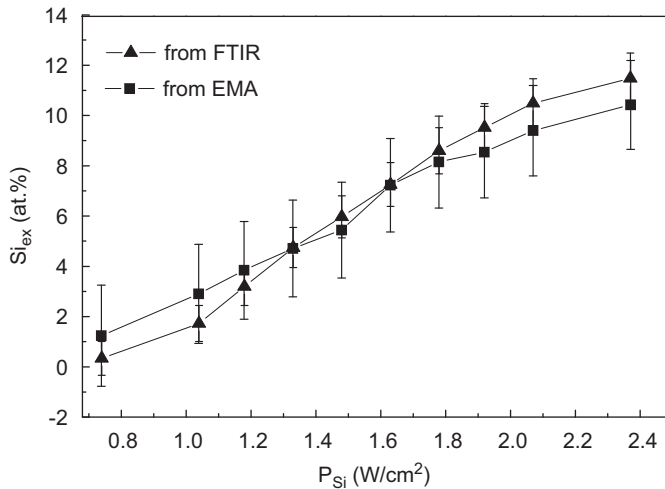


Fig. 2. Evolution of Si_{ex} (at.%) as a function of P_{Si} for as-deposited samples.

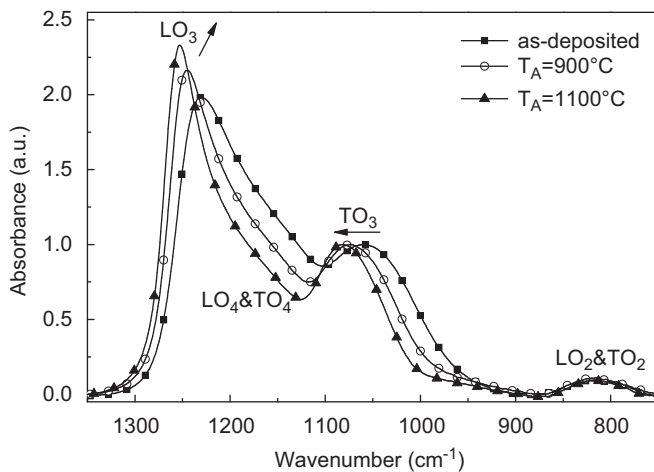


Fig. 3. Typical evolution of the FTIR spectra measured in Brewster incidence for as-deposited and annealed films.

3.3. Photoluminescence properties

The film with $P_{\text{Si}}=1.33 \text{ W/cm}^2$ was once more chosen to demonstrate the evolution of light emission properties versus an annealing treatment. The room temperature PL spectra of sample as-deposited and annealed at 900 and 1100 °C are shown in Fig. 4. It is seen that the sample annealed at 1100 °C emits a broad PL band in the visible domain that can be ascribed to radiative carrier recombination in Si-ncs.

As one can also see from Fig. 4, no emission was detected in this range for both as-deposited and 900 °C-annealed sample. However, this latter FTIR spectrum (Fig. 3) shows a phase separation process and thus the presence of Si-ncs. We conclude that the visible emission is quenched either due to energy transfer or to defect in the host [28]. This assumption is confirmed by the analysis of the Nd^{3+} PL bands (Fig. 4).

In the infrared domain, there are peaks centered at around 920 nm corresponding to the intra-4f shell transition of Nd^{3+} ions from the $^4\text{F}_{3/2}$ to the $^4\text{I}_{9/2}$ level. The presence of the PL of Nd^{3+} ions after non-resonant excitation at 488 nm confirms the sensitizing effect of Si-ncs toward Nd^{3+} ions. Moreover, the most efficient emission is observed for the sample annealed at 900 °C which corresponds to the best coupling between Si-ncs and Nd^{3+} ions. It is worth to note that a notable emission from Nd^{3+} ions

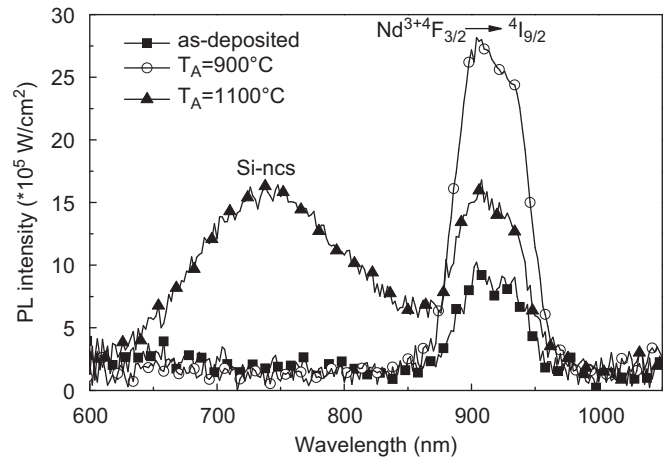


Fig. 4. Typical evolution of the PL spectra of sample with $P_{\text{Si}}=1.33 \text{ W/cm}^2$ for as-deposited and annealed films.

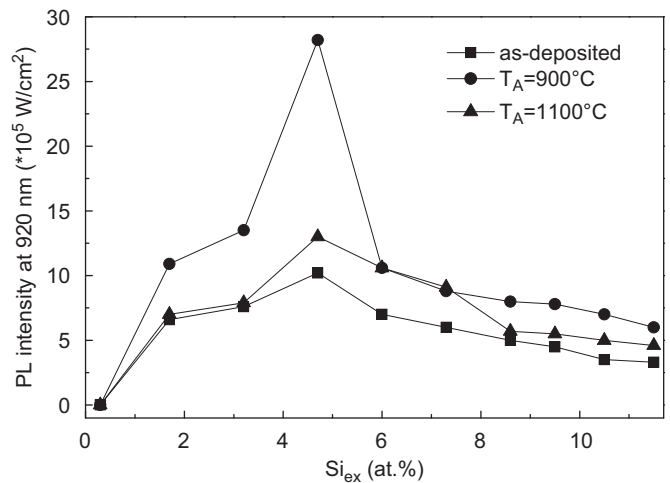


Fig. 5. Evolution of the Nd^{3+} PL intensity at 920 nm as a function of the P_{Si} for as-deposited and annealed films.

was obtained for the as-deposited sample and this fact can be explained by either formation of Si-ncs during fabrication process or by energy transfer from host defects towards RE ions [19].

In the following part, the effect of Si_{ex} on Nd^{3+} PL properties will be studied as shown in Fig. 5. The Nd^{3+} PL intensity shows first an increase with Si_{ex} for all as-deposited and annealed samples, up to a maximum corresponding to sample with $\text{Si}_{\text{ex}}=4.7\%$ ($P_{\text{Si}}=1.33 \text{ W/cm}^2$), and then decreases for higher Si_{ex} . This behavior may be explained by two reasons. On one hand, the first increase of Si_{ex} is expected to enhance the density of Si-ncs for an optimized Nd^{3+} :Si-ncs interaction. Further increase of Si_{ex} up to 11.5 at% might lead to increasing the average size of the former Si-ncs at the expense of their density and then of their coupling with Nd^{3+} ions. On the other hand, the Si incorporated into the sample may result in disorder in the host, which will favor the non-radiative channels. Besides in Fig. 5, the samples annealed at 900 °C show the highest PL intensity whatever the Si_{ex} . This observation may be ascribed to the formation of Nd_2O_3 clusters [17] for samples after annealing at high temperature ($T_{\text{A}}=1100 \text{ °C}$). To note that there is no peak for sample with $\text{Si}_{\text{ex}}=0.3 \text{ at.}\%$, possibly because the emission is too weak to be detected for the low Si_{ex} , the Nd^{3+} :Si-ncs distance is too high to allow the energy transfer process.

4. Conclusion

We have investigated the influences of Si_{ex} and T_A on the structure and optical properties of Nd-doped SRSO thin films fabricated by co-sputtering technique. It has been shown that the increase in Si_{ex} improves the Si-ncs coupling to Nd^{3+} ions, and that, it may raise the disorder in layer resulting in the increase of the number of non-radiative channels. In addition, it has been evidenced that the post annealing treatment at 900 and 1100 °C enhances the layer quality favoring the Nd^{3+} PL emission. However, high temperature annealing leads to a decrease of the Nd^{3+} emission due to the coalescence of Si-ncs and/or the formation of Nd_2O_3 cluster. Therefore, both moderate T_A and Si_{ex} are very important to be found with aim to optimize the emission from Nd^{3+} ions. In this study, the sample with $Si_{ex}=4.7$ at% ($P_{Si}=1.33$ W/cm²) shows the highest Nd^{3+} peaks after annealing at 900 °C for 1 h.

Acknowledgments

The authors thank the French National Agency (ANR), which supported this work through the Nanoscience and Nanotechnology program (DAPHNES project ANR-08-NANO-005).

References

- [1] A. Polman, B. Min, J. Kalkman, T.J. Kippenberg, K.J. Vahala, *Appl. Phys. Lett.* 84 (2004) 1037.
- [2] A.J. Kenyon, *Semicond. Sci. Technol.* 20 (2005) R65.
- [3] L. Dal Negro, J.H. Yi, J. Michel, L.C. Kimerling, S. Hamel, A. Williamson, G. Galli, *IEEE J. Sel. Top. Quantum Electron.* 12 (2006) 1628.
- [4] M. Fujii, M. Yoshida, Y. Kanzawa, S. Hayashi, K. Yamamoto, *Appl. Phys. Lett.* 71 (1997) 1198.
- [5] A.J. Kenyon, P.F. Trwoga, M. Federighi, C.W. Pitt, *J. Phys.: Condens. Matter* 6 (1994) L319.
- [6] S. Charvet, R. Madelon, F. Gourbilleau, R. Rizk, *J. Lumin.* 80 (1998) 257.
- [7] S. Cuffe, C. Labbe', B. Dierre, F. Fabbri, T. Sekiguchi, X. Portier, R. Rizk, *J. Appl. Phys.* 108 (2010) 113504.
- [8] C.W. Thiel, T. Böttger, R.L. Cone, *J. Lumin.* 131 (2011) 353.
- [9] K. Watanabe, M. Fujii, S. Hayashi, *J. Appl. Phys.* 90 (2001) 4761.
- [10] G. Franzò, S. Bonitelli, D. Pacifici, F. Priolo, F. Iacona, C. Bongiorno, *Appl. Phys. Lett.* 82 (2003) 3871.
- [11] F.D. Pacifici, G. Franzò, F. Priolo, F. Iacona, L. Dal Negro, *Phys. Rev. B* 67 (2003) 245301.
- [12] F. Gourbilleau, M. Levalois, C. Dufour, J. Vicens, R. Rizk, *J. Appl. Phys.* 95 (2004) 3717.
- [13] C. Garcia, P. Pellegrino, Y. Lebour, B. Garrido, F. Gourbilleau, R. Rizk, *J. Lumin.* 121 (2006) 204.
- [14] P. Pellegrino, B. Garrido, J. Arbiol, C. García, Y. Lebour, J.R. Morante, *Appl. Phys. Lett.* 88 (2006) 121915.
- [15] K. Hijazi, R. Rizk, J. Cardin, L. Khomenkova, F. Gourbilleau, *J. Appl. Phys.* 106 (2009) 024311.
- [16] F. Gourbilleau, R. Madelon, C. Dufour, R. Rizk, *Opt. Mater.* 27 (2005) 868.
- [17] O. Debieu, D. Bréard, A. Podhorodecki, G. Zatoryb, J. Misiewicz, C. Labbé, J. Cardin, F. Gourbilleau, *J. Appl. Phys.* 108 (2010) 113114.
- [18] D. Bréard, F. Gourbilleau, C. Dufour, R. Rizk, J.-L. Doualan, P. Camy, *Mater. Sci. Eng. B.* 146 (2008) 179.
- [19] S. Cuffe, C. Labbé, O. Jambois, B. Garrido, X. Portier, R. Rizk, *Nanoscale Res. Lett.* 6 (2011) 395.
- [20] <<http://www.horiba.com/scientific/products/ellipsometers/software/>>.
- [21] D.E. Aspnes, *Thin Solid Films* 89 (1982) 249.
- [22] E. Dehan, P. Temple-Boyer, R. Henda, J.J. Pedroviejo, E. Scheid, *Thin Solid Films* 266 (1995) 14.
- [23] L. Khomenkova, X. Portier, J. Cardin, F. Gourbilleau, *Nanotechnology* 21 (2010) 285707.
- [24] B.J. Hinds, F. Wang, D.M. Wolfe, C.L. Hinkle, G. Lucovsky, *J. Non-Cryst. Solids* 227–230 (1998) 507.
- [25] S. Charvet, R. Madelon, F. Gourbilleau, R. Rizk, *J. Appl. Phys.* 85 (1999) 4032.
- [26] H. Ono, T. Ikarashi, K. Ando, T. Kitano, *J. Appl. Phys.* 84 (1998) 6064.
- [27] F. Gourbilleau, C. Dufour, M. Levalois, J. Vicens, R. Rizk, C. Sada, F. Enrichi, G. Battaglin, *J. Appl. Phys.* 94 (2003) 3869.
- [28] L. Skuja, *J. Non-Cryst. Solids* 239 (1998) 16.